Benchmark study of DFT and composite methods for bond dissociation energies in argon compounds

Li-Juan Yu,[a,d,*] Stephen G. Dale,[b] Bun Chan,[c] Amir Karton[d,*]

[a]ARC Centre of Excellence for Electromaterials Science, Research School of Chemistry, Australian National University, Canberra, Australian Capital Territory 2601, Australia

[b]The School of Chemistry, The University of Sydney, Sydney, New South Wales 2006, Australia

[c]Graduate School of Engineering, Nagasaki University, Bunkyo 1-14, Nagasaki-shi, Nagasaki 852-8521, Japan

[d]School of Molecular Sciences, The University of Western Australia, Perth, Western Australia 6009 Australia

Abstract

We introduce a database of 14 accurate bond dissociation energies (BDEs) of noble gas compounds. Reference CCSD(T)/CBS BDEs are obtained by means of W1 theory. We evaluate the performance of 65 contemporary density functional theory (DFT) and double-hybrid DFT (DHDFT) procedures. A general improvement in performance is observed along the rungs of Jacob's Ladder; however, only a handful of functionals give good performance for predicting the bond dissociation energies in the NGC14 database. Thus, this database represents a challenging test for DFT methods. Most of the conventional DFT functionals (71%) result in root-mean-square deviations (RMSDs) between 10.0 and 82.1 kJ mol^{-1}. The rest of the DFT functionals attain RMSDs between 2.5 and 8.9 kJ mol^{-1}. The best performing functionals from each rung of Jacob's Ladder are (RMSD given in parenthesis): HCTH407 (30.9); M06-L (5.4); PBE0 (2.8); B1B95, M06, and PW6B95 (2.7–2.9); CAM-B3LYP-D3 (5.4); and B2T-PLYP (2.5 kJ mol^{-1}). The NGC14 dataset also proves to be a non-trivial target for approximate composite ab initio procedures.

Corresponding Authors E-mail address: lijuan.yu@anu.edu.au (L.-J. Yu) and amir.karton@uwa.edu.au (A. Karton).

Cite as:
L.-J. Yu, S. G. Dale, B. Chan, A. Karton, Chem. Phys. 531, 110676 (2020).
https://doi.org/10.1016/j.chemphys.2019.110676

1. Introduction

The noble gases are a remarkable group of elements. They are generally inert due to their stable electronic structures and it is uncommon that they form stable chemical bonds at room temperature. The first inert gas was isolated by Ramsay and Rayleigh in 1895 and it was named argon. It constitutes 0.934% by volume and 1.288% by mass of the earth's atmosphere. The other noble gases were isolated afterwards. In 1933 Pauling predicted that the heavier noble gases could form stable molecules since their valence electrons are screened from the nucleolus by core electrons and thus less strongly bound.[1] This prediction was verified by the preparation of the first compound containing a noble gas atom, $XePtF_6$.[2] Since then, a range of compounds containing xenon[3-10], krypton[5, 11-12] and radon,[13-14] have been prepared. Chemical bonding of the noble gases has previously been limited to the heavier elements, e.g. krypton, xenon, and radon. The prospects of chemical bonding for the lighter noble gases are far poorer since the stability of the ground state electronic configurations of these atoms is much greater. In 2000, a first stable chemically bound compound of argon, HArF, was prepared experimentally in a low temperature Ar matrix.[15] The preparation of HArF is therefore an important advance that opens the potential to study the chemistry of argon.

Over the past two decades, density functional theory (DFT) has become the dominant electronic structure method in materials and quantum chemistry due to its attractive accuracy-to-computational cost ratio. Contemporary DFT methods are demonstrated to be successful in many areas of theoretical chemistry, but their performance must always be cautiously verified. Kohn–Sham DFT is exact in principle, but it involves an unknown exchange-correlation (XC) functional, which has to be approximated.[16] Developing improved approximations for the XC functional is a major ongoing research area.[17-19] Despite significant advances in DFT methodology development in the past decades, the various XC approximations often exhibit

widely different performances for different chemical properties. This situation leads to a practical problem in the application of DFT methods to a given chemical problem. Jacob's Ladder of DFT is a useful scheme, where various XC functionals are grouped on sequential rungs on a ladder, with each rung representing improved accuracy.[20] While the accuracy of DFT increases as one climbs up the rungs of Jacob's Ladder, at present, no truly systematic path toward the exact XC functional exists. Thus, the only validation of a given DFT method for a given chemical problem (e.g. weak interactions and bond dissociation energies) is benchmarking against accurate reference data. In particular, the performance of DFT and other more approximate composite procedures has been extensively examined for bond dissociations energies (BDEs). Johnson *et al.*[21] examined X–H, X–X and X–Y bonds (X, Y = C, N, O, F, S, Cl and Br) and identified particularly poor performance for delocalized systems including functional groups with multiple bonds. Izgorodina *et al.*[22] showed the mean absolute deviations (MADs) for the DFT methods in predicting the BDEs of C–X (X = H, C, O and F) range from 7.0–8.0 kJ mol^{-1} to around 30.0 kJ mol^{-1}, while the composite methods (e.g. G3-RAD, G3(MP2)-RAD) show good performance in predicting these BDEs with MAD of around 3.0 kJ mol^{-1}. Chan and Radom evaluated the performance of DFT, double-hybrid DFT (DHDFT), and high-level composite procedures for calculating 261 BDEs for bonds between hydrogen, first-row and second-row p-block elements.[23] They demonstrated that the deviations of BDEs for the traditional DFT methods are systematically underestimated, while DHDFT generally give smaller deviations for BDEs and composite methods show even better performance. The BDEs of both N–H and N–Cl bonds represent a challenge for DFT procedures, while the G*n* type methods perform better but systematically underestimate the N–X BDEs.[24] For the N–Br BDE, over 90% of the tested DFT functionals have RMSDs that are larger than 10.0 kJ mol^{-1}.[25] For the BDE99 dataset of 99 bond dissociation reactions, again traditional DFT procedures perform poorly with RMSDs up to

~45.0 kJ mol^{-1} and DHDFT give better performance with RMSDs up to 14.0 kJ mol^{-1}. Even composite procedures attain RMSDs up to 8.0 kJ mol^{-1} for this dataset.[26]

Noble gas compounds, such as HArF, constitute some of the most unusual and surprising examples of chemical bonding.[27] It is therefore of interest to test the performance of various DFT methods for the chemistry of noble gas compounds. In the present study, we introduce a representative database including 14 noble gas compounds containing argon and fluorine, FArR, where R is either electron-donating group or electron-withdrawing group. We calculate the FAr–R BDEs at the CCSD(T)/CBS level by means of the high-level W1 protocol. We use these accurate BDEs to assess the performance of a wide range of DFT procedures from rungs 2–5 of Jacob's ladder for the BDE of the FAr–R bond. Specifically, we examine the performance of a variety of contemporary DFT procedures, including DHDFT and a number of more approximate composite methods.

2. Computational details

To obtain reliable reference BDEs for the database, calculations have been carried out at the CCSD(T)/CBS level of theory[28-29] (i.e., coupled cluster with single, double, and quasiperturbative triple excitations at the complete basis set limit) with the Molpro 2012.1 program suite.[30] The Hartree–Fock (HF), CCSD, (T) and core-valence (CV) energies are obtained from W1 theory.[31-32] Specifically, the HF component is extrapolated from the A'VTZ and A'VQZ basis sets using the $E(L) = E_\infty + A/L^\alpha$ two-point extrapolation formula with $\alpha = 5$ (A'VnZ indicates the combination of the standard correlation-consistent cc-pVnZ basis sets[33] on H and aug-cc-pVnZ basis sets[34] on first-row atoms and aug-cc-pV(n+d)Z basis sets[35] on second-row atoms). The CCSD correlation energy is extrapolated from the same basis sets with an extrapolation exponent of $\alpha = 3.22$. The (T) correlation component is extrapolated from the A'VDZ and A'VTZ basis sets with $\alpha = 3.22$ as well. Core-valence

corrections have been calculated at the CCSD(T) level in conjunction with the cc-pwCVTZ basis set.[36]

The geometries were obtained at the B3LYP-D3/aug-cc-pVTZ level of theory.[37-44] Empirical D3 dispersion corrections[41-42, 44] are included using Becke–Johnson damping potential[43] as recommended in Ref. 40 (denoted by the suffix -D3). We note that the suffix -D in B97-D and ωB97X-D indicates the original dispersion correction rather than the D3 correction. Harmonic vibrational analyses have been performed to confirm each stationary point as an equilibrium structure (i.e., all real frequencies). All geometry optimizations and frequency calculations were carried out using Gaussian 09, Revision E.01.[45]

The DFT XC functionals considered in the present study (ordered by their rung on Jacob's Ladder) are the generalized gradient approximation (GGA) functionals: BLYP,[37, 46] B97-D,[44] HCTH407,[47] PBE,[48] BP86,[46, 49] BPW91,[46, 50] SOGGA11,[51] we also consider the non-separable gradient approximation (NGA) functional N12;[52] the meta-GGAs (MGGAs): M06-L,[53] TPSS,[54] τ-HCTH,[55] VSXC,[56] BB95,[57] M11-L,[58] we also consider the meta-NGA functional MN12-L;[59] the hybrid-GGAs(HGGAs): BH&HLYP,[60] B3LYP,[37-39] B3P86,[38, 49] B3PW91,[38, 50] PBE0,[61] B97-1,[62] B98,[63] X3LYP,[64] SOGGA11-X;[65] the hybrid-meta-GGAs (HMGGAs): M05,[66] M05-2X,[67] M06,[68] M06-2X,[68] M06-HF,[68] BMK,[69] B1B95,[46, 57] TPSSh,[70] τ-HCTHh,[55] PW6B95,[71] and the double-hybrid DFT procedures (DHDFT): B2-PLYP,[72] B2GP-PLYP,[73] B2K-PLYP,[74] B2T-PLYP,[74] DSD-BLYP,[75] DSD-PBEP86,[76-77] PWPB95.[78] We also considered the following range-separated (RS) functionals: CAM-B3LYP,[79] LC-ωPBE,[80] ωB97,[81] ωB97X,[81] ωB97X-D,[82] and M11.[83] The performance of the DFT was investigated in conjunction with the A'VTZ correlation-consistent basis set of Dunning's, while the DHDFT calculations, which exhibit slower basis set convergence, were carried out in conjunction with A'VQZ basis set. In addition, the performance of composite thermochemical procedures

was also assessed. We considered the following composite procedures: G3,[84] G3(MP2),[85] G3B3,[86] G3MP2B3,[86] G4,[87] G4(MP2),[88] G4(MP2)-6X,[89] and CBS-QB3.[90]

3. Results and discussion

3.1 Benchmark bond dissociation energies for the NGC14 dataset

The NGC14 dataset contains the following 14 (shown in Figure 1) bond dissociation energies:

$$F–Ar–R \rightarrow F–Ar\bullet + \bullet R$$

Where R = H (1), $CHCH_2$ (2), C_6H_5 (3), C_6H_4Y (Y=CCH (4), CHO (5), Cl (6), CN (7), COOH (8), F (9), NH_2 (10), NO_2 (11), OH (12), OMe (13), and NMe_2 (14)). The substitutions on phenyl are at the para position. All the reactions involve breaking the Ar–C bond except for R = H.

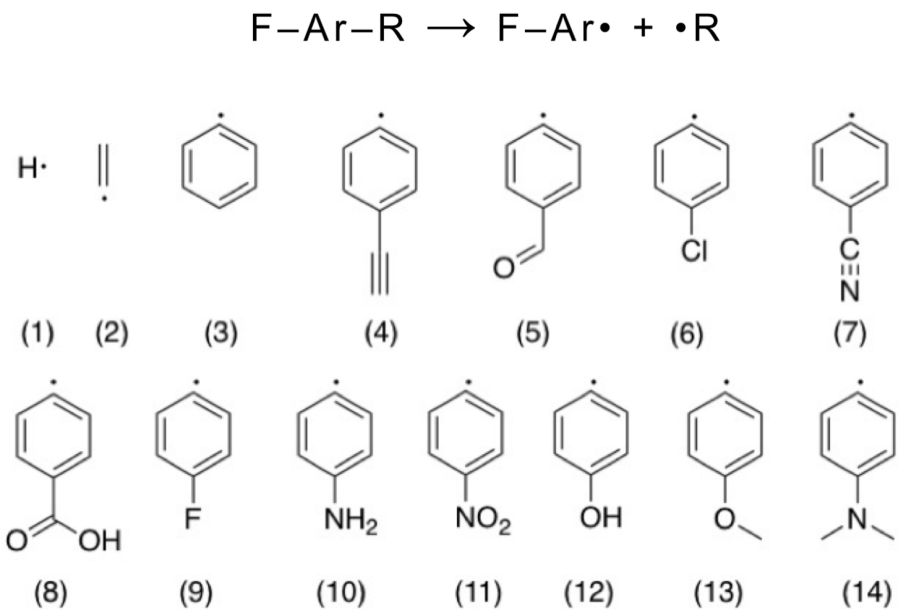

Figure 1. Bond dissociation reactions in the NGC14 dataset.

The component breakdown of the benchmark CCSD(T)/CBS bond dissociation energies are gathered in Table 1. The HF/CBS level systematically highly underestimates the

CCSD(T)/CBS bond dissociation energies. Thus, complete neglect of the electron correlation would lead to systematic underestimation of the bond dissociation energies. The CCSD/CBS level underestimates the bond dissociation energies systematically in this dataset as well. The (T) correction plays significant role in predicting the bond dissociation energies for this dataset. The core valence correction plays a minor role for the bond dissociation energies in this dataset.

Table 1. Component breakdown of the benchmark CCSD(T)/CBS bond dissociation energies in the NGC14 dataset (W1 theory, kJ mol^{-1}).

Reaction	HF	ΔCCSD	Δ(T)	CV	CCSD(T)
1	-219.7	233.4	30.2	0.0	43.9
2	-241.1	223.9	44.1	0.0	26.8
3	-234.1	227.2	44.7	0.3	38.0
4	-241.5	230.3	45.6	0.3	34.6
5	-250.6	233.5	46.2	0.2	29.3
6	-243.7	230.8	45.7	0.3	33.0
7	-259.5	236.2	47.5	0.2	24.5
8	-248.5	233.0	46.1	0.3	30.9
9	-240.1	229.2	45.3	0.3	34.6
10	-219.6	222.8	42.9	0.5	46.6
11	-263.2	238.5	48.0	0.2	23.6
12	-228.2	225.4	43.9	0.3	41.4
13	-231.3	225.6	43.6	0.3	38.2
14	-214.2	222.0	42.4	0.5	50.7

As our reference BDEs are obtained at the CCSD(T)/CBS level of theory, it is of interest to estimate whether post-CCSD(T) contributions are likely to be significant. The percentage of the total atomization energy (TAE) accounted for by parenthetical connected triple excitations, %TAE[(T)], has been shown to be reliable energy-based diagnostic for the importance of non-dynamical correlation effects.[26, 29, 91] Table S1 (Supporting Information) gathers the %TAE[(T)] values for the FArR systems considered in the present work. The %TAE[(T)] values range between 1.6 (FArH) and 4.0 ($FArC_6H_4NO_2$). It has been found that %TAE[(T)] ≤ 5% indicated that the post-CCSD(T) contributions to the TAEs should be

on the order of 1–4 kJ mol^{-1}.[29] For the smallest systems in the dataset HArF and FArCHCH$_2$ we were able to calculate the post-CCSD(T) contributions explicitly from W3.2 theory.[91] In particular, the CCSDT–CCSD(T) component is extrapolated from the cc-pVDZ and cc-pVTZ basis sets and amounts to –1.6 (HArF) and –2.4 (FArCHCH$_2$) kJ mol^{-1}. The CCSDT(Q)–CCSDT component is calculated in conjunction with the cc-pVDZ basis set and amounts to 2.1 (HArF) and 5.5 (FArCHCH$_2$) kJ mol^{-1}. Thus, overall the post-CCSD(T) contributions to the BDEs are 1.6 (HArF) and 3.2 (FArCHCH$_2$) kJ mol^{-1}.

3.2 Performance of DFT for the bond dissociation energies in the NGC14 dataset

The CCSD(T)/CBS bond dissociation energies provide a benchmark set of values for the assessment of the performance of DFT procedures for the calculation of Ar–R bond dissociation energies. For a rigorous comparison with the DFT results, secondary effects that are not explicitly included in the DFT calculations, such as zero-point vibrational corrections, are not included in the reference values. Table 2 shows the root-mean-square deviation (RMSD), mean-absolute deviation (MAD), and mean-signed deviation (MSD) from our benchmark W1 results for various contemporary DFT functionals with and without empirical D3 dispersion corrections.

General improvement in performance along the rungs of Jacob's Ladder. Inspection of the error statistics in Table 2 reveals that there is a general improvement in the performance of the DFT functionals along the rungs of Jacob's Ladder, except for some of the HMGGA functional where the percentage of exact HF exchange is high. The RMSDs for the GGA methods (rung 2) spread over a wide range from 30.9 (HCTH407) to 73.6 (BP86-D3) kJ mol^{-1} with an average RMSD of 53.7 kJ mol^{-1} for all the GGA functionals considered here. None of the considered GGA methods results in RMSDs close to the threshold of "chemical

accuracy" (defined here as RMSD < 4.0 kJ mol^{-1}). For the MGGA methods (rung 3), the RMSDs range between 5.4 (M06-L) and 68.6 (BB95) kJ mol^{-1} with an average RMSD of 28.1 kJ mol^{-1} for all the considered MGGA functionals. The HGGA functionals (with an average RMSD of 20.5 kJ mol^{-1}) except for BH&HLYP (which is associated with an RMSD of 82.1 kJ mol^{-1}) give better performance with RMSDs ranging between 2.8 (PBE0) and 26.0 (SOGGA11-X) kJ mol^{-1}. The HMGGA methods (rung 4) (with an average RMSD of 11.5 kJ mol^{-1}), with the percentage of HF exchange ranging between 10% and 100%, show a wide range of RMSDs. The best performer B1B95 results in an RMSD of 2.7 kJ mol^{-1}. The range-separated methods show somewhat disappointing performance, with RMSDs between 5.4 (CAM-B3LYP-D3) and 25.6 (LC-ωPBE) kJ mol^{-1}. Half of the considered double-hybrid methods (rung 5) give good performance, particularly B2GP-PLYP, B2K-PLYP, B2T-PLYP and PWPB95 resulting in RMSDs below the chemical accuracy threshold.

GGA and MGGA methods significantly overestimate the BDEs in the NGC14 database. Table 2 shows that all the GGA methods systematically overestimate the bond dissociation energies in the dataset, as evident from MSD = MAD. This is illustrated graphically in Figure 2. The MSDs range from 30.7 (HCTH407) to 73.3 (PBE-D3) kJ mol^{-1}. The GGA procedures show particularly poor performance for the BDEs in reactions 1 and 13.

The inclusion of the kinetic energy density in the MGGA functionals improves the situation to some extent. However, the MGGAs still overestimate or underestimate the bond dissociation energies by up to 70 kJ mol^{-1}. Reactions in the NGC14 dataset prove to be very challenging for all the considered MGGA procedures except for M06-L, which results in an RMSD of 5.4 kJ mol^{-1}.

Table 2. Statistical analysis for the performance of DFT procedures for the calculation of the bond dissociation energies in the NGC14 database (in kJ mol^{-1}).[a,b]

Type[c]	Procedure	RMSD	MAD	MSD	LD[d]
GGA	BLYP	44.4	44.3	44.3	50.7(1)
	BLYP-D3	56.6	56.5	56.5	61.4(13)
	B97-D	35.9	35.8	35.8	45.6(1)
	B97-D3	43.1	43.1	43.1	48.6(1)
	HCTH407	30.9	30.7	30.7	42.7(1)
	PBE	67.5	67.4	67.4	72.7(2)
	PBE-D3	73.4	73.3	73.3	78.5(13)
	BP86	63.7	63.6	63.6	71.1(1)
	BP86-D3	73.6	73.6	73.6	78.0(13)
	BPW91	50.2	50.2	50.2	55.5(2)
	SOGGA11	47.9	47.8	47.8	52.7(2)
	N12[e]	57.5	57.4	57.4	62.8(13)
MGGA	M06-L	5.4	5.0	5.0	10.3(2)
	TPSS	34.9	34.7	34.7	42.6(1)
	TPSS-D3	42.4	42.4	42.4	46.9(13)
	τ-HCTH	38.6	38.5	38.5	47.6(1)
	VSXC	6.4	5.1	5.1	17.1(1)
	BB95	68.6	68.5	68.5	74.6(2)
	M11-L	19.5	19.2	-17.9	22.5(14)
	MN12-L[e]	8.9	8.5	-8.0	11.7(11)
HGGA	BH&HLYP	82.1	81.9	-81.9	89.3(11)
	BH&HLYP-D3	74.0	73.8	-73.8	80.6(11)
	B3LYP	4.7	2.8	2.5	14.6(1)
	B3LYP-D3	12.8	12.6	12.6	18.1(13)
	B3P86	20.8	20.4	20.4	33.0(1)
	B3PW91	4.9	3.8	3.8	12.1(1)
	B3PW91-D3	14.4	14.3	14.3	19.9(13)
	PBE0	2.8	2.5	-1.8	4.4(5)
	PBE0-D3	4.2	3.6	3.6	9.5(13)
	B97-1	10.7	10.3	10.3	16.1(13)
	B98	5.6	5.1	5.1	10.4(13)
	X3LYP	4.0	2.4	1.5	12.1(1)
	SOGGA11-X	26.0	25.8	-25.8	29.7(11)
HMGGA	M05	13.3	12.9	-12.9	17.0(11)
	M05-2X	11.4	11.0	-11.0	15.4(11)
	M06	2.9	2.2	1.1	6.6(13)
	M06-2X	26.2	26.1	-26.1	30.6(11)
	M06-HF	24.1	23.8	-23.8	31.0(11)
	BMK	14.5	14.1	-14.1	19.2(1)
	BMK-D3	7.7	6.5	-6.3	18.4(1)
	B1B95	2.7	2.4	-1.2	4.3(11)
	B1B95-D3	7.2	6.8	6.8	13.1(13)
	TPSSh	10.3	9.5	9.5	21.5(1)

	τ-HCTHh	22.9	22.8	22.8	28.1(13)
	PW6B95	2.9	2.5	-1.6	4.9(11)
	PW6B95-D3	3.1	2.2	2.0	8.0(13)
RS	CAM-B3LYP	10.5	9.9	-9.7	14.4(11)
	CAM-B3LYP-D3	5.4	5.0	-4.3	8.5(11)
	LC-ωPBE	25.6	25.3	-25.3	30.2(11)
	LC-ωPBE-D3	19.5	19.2	-19.2	23.6(11)
	ωB97	20.1	19.8	-19.8	24.4(11)
	ωB97X	20.2	20.0	-20.0	24.3(11)
	ωB97X-D	11.4	11.1	-11.1	14.5(11)
	M11	8.0	7.1	-6.8	12.5(11)
DH	B2-PLYP	12.0	12.0	12.0	17.0(13)
	B2-PLYP-D3	18.5	18.4	18.4	24.1(13)
	B2GP-PLYP	2.8	2.4	2.0	7.5(13)
	B2GP-PLYP-D3	6.5	6.1	5.9	11.8(13)
	B2K-PLYP	3.4	2.2	-1.2	8.9(1)
	B2T-PLYP	2.5	2.0	2.0	7.3(13)
	DSD-BLYP	12.9	12.4	12.4	17.8(13)
	DSD-PBEP86	15.9	15.1	15.1	20.4(13)
	DSD-PBEP86-D3	20.0	19.2	19.2	24.8(13)
	PWPB95	3.0	2.5	2.2	7.7(13)
	PWPB95-D3	5.6	5.3	5.0	10.8(13)

[a]The standard DFT calculations are carried out in conjunction with the A'VTZ basis set while the DHDFT calculations are carried out in conjunction with the A'VQZ basis set.
[b]RMSD = root mean square deviation, MAD = mean absolute deviation, MSD = mean signed deviation, LD = largest deviation (in absolute value).
[c]GGA = generalized gradient approximation, HGGA = hybrid-GGA, MGGA = meta-GGA, HMGGA = hybrid-meta-GGA, RS = range-separated, DH = double hybrid.
[d]The reaction numbers are given in parenthesis.
[e]N12 and MN12 are non-separable gradient approximation (NGA) and meta-NGA functionals, respectively.

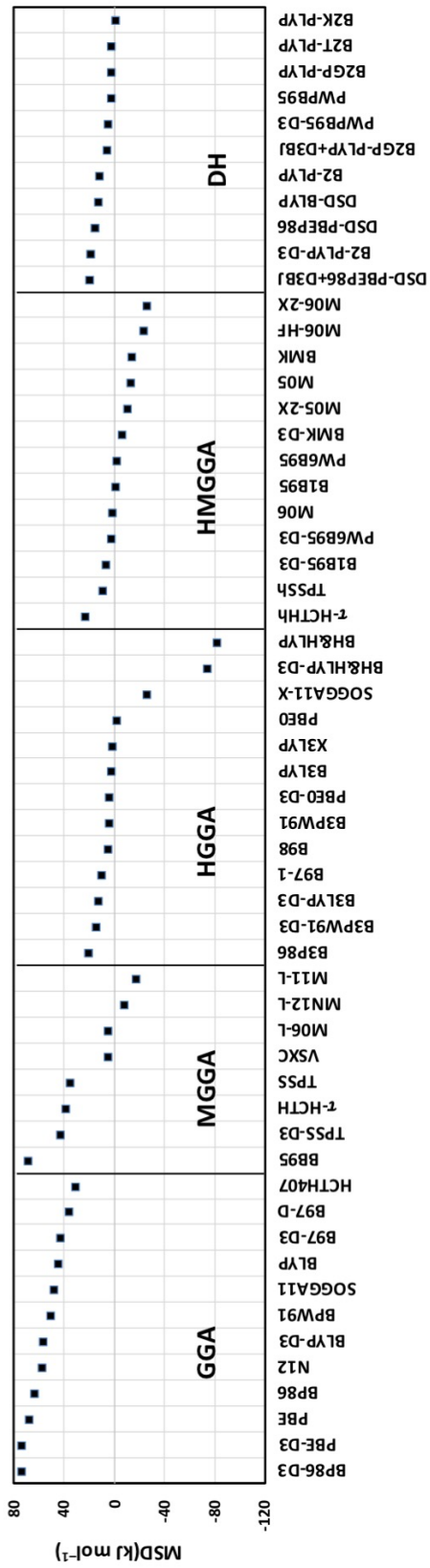

Figure 2. Mean-signed deviations (MSDs) for the DFT procedures over the bond dissociation energies in the NGC14 database (in kJ mol^{-1}). The MSDs for all the DFT procedures are given in Table 2.

Most hybrid and hybrid-MGGAs show good performance. The performance of the 13 HGGA and 13 HMGGA functionals considered here vary significantly. The RMSDs for these rung 4 functionals range between 2.7 (B1B95) and 82.1 (BH&HLYP) kJ mol^{-1}. The BH&HLYP is associated with an RMSD of 82.1 kJ mol^{-1}. Inspection of the MSDs in Figure 2 and Table 2 reveals that a general correlation between the amount of exact HF exchange (%HF) and the functional's MSD values. The functionals with the largest MSDs incorporate about 28–100% of exact HF exchange. For example, hybrid functionals with 40–50% of exact HF exchange (e.g., SOGGA11-X and BH&HLYP) are associated with MSDs between –25.8 and –81.9 kJ mol^{-1}. Hybrid-MGGA functionals with < 20% and 40–100% of exact exchange (e.g., TPSSh, τ-HCTHh, M05, BMK, M05-2X, M06-2X and M06-HF) are associated with MSDs between –11.0 and –81.9 kJ mol^{-1}. However, functionals with 20–28% of exact exchange (e.g. B3LYP, B3PW91, PBE0, B98 and X3LYP) are associated with near-zero MSDs.

Figure 3 illustrates the relationship between the percentage of exact HF exchange and the MSDs for the 26 HGGA and HMGGA functionals. For a meaningful comparison, dispersion-corrected functionals are not included in the plot and will be discussed separately in a following section. It is obvious that functionals with 40–100% of exact exchange are associated with very large MSDs ranging from –11.0 to –81.9 kJ mol^{-1}. Five functionals X3LYP, PBE0, M06, B1B95, and PW6B95 with 22%, 25%, 27%, 28% and 28% exact HF exchange respectively give best performance with near-zero MSDs. Functionals with more than 28% of exact HF exchange are associated with more negative MSDs, which means the bond dissociation energies are highly underestimated with more exact HF exchange included in the functionals.

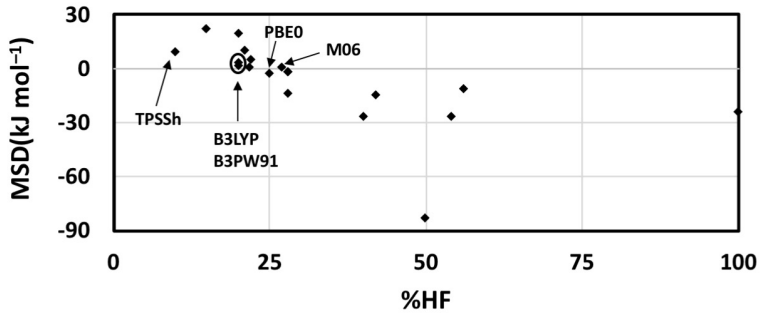

Figure 3. Relationship between MSDs over the NGC14 dataset and the percentage of exact HF exchange (%HF) mixing coefficient for the hybrid and hybrid-meta GGA functionals. The MSDs are taken from Table 2.

Finally, it is constructive to compare the performance of the three hybrid functionals B3LYP, B3P86 and B3PW91, which combine Becke's three-parameter exchange functional with different gradient-corrected correlation functionals. These functionals give RMSDs of 4.7, 20.8 and 4.9 kJ mol^{-1}, respectively. Thus, the P86 correlation functional is worse than PW91 and LYP functionals for this dataset.

Optimal percentage of exact HF exchange. The results of the previous section show that functionals with 25–100% of exact HF exchange tend to underestimate the bond dissociation energies in the NGC14 dataset. While the functionals with 10–22% of exact HF exchange tend to overestimate the BDEs in the NGC14 dataset. Thus, the optimal percentage of exact HF exchange seems to lie in between 20%–30%. To investigate this further, we choose three GGAs (BLYP, BP86 and PBE) and two MGGAs (TPSS and τ-HCTH) and scan the percentage of exact HF exchange (%HF). The MSDs and RMSDs for the dataset are depicted in Figure 4. It can be seen that for all five functionals the MSD varies linearly along the percentage of exact HF exchange in the functional. Very low percentage of exact HF exchange leads to large positive MSDs of up to 67.4 kJ mol^{-1}. The MSD curve crosses the x-

axis at ~15–25% of exact HF exchange for all five functionals (consistent with the results in Figure 3). We note that Zhang and Schwarz found that an admixture of ~20–30% exact HF exchange is required for obtaining a good description of BDEs of M^+–OH*n* systems (M = K – La, Hf – Rn; *n* = 0–2).[92] While high percentage of exact HF exchange leads to large negative MSDs of up to around –200 kJ mol^{-1}. Figure 4 also shows that at the exact HF exchange percentage for which the MSDs are near zero, all the functionals result in small RMSDs. In particular, the RMSDs are 3.9 (BLYP with 18% HF exchange), 2.8 (PBE with 25% HF exchange), 4.9 (BP86 with 25% HF exchange), 4.4 (TPSS with 14% HF exchange) and 3.8 (τ-HCTH with 14% HF exchange) kJ mol^{-1}. For the details of the percentage of exact HF exchange, see Figure S1 in the Supporting Information.

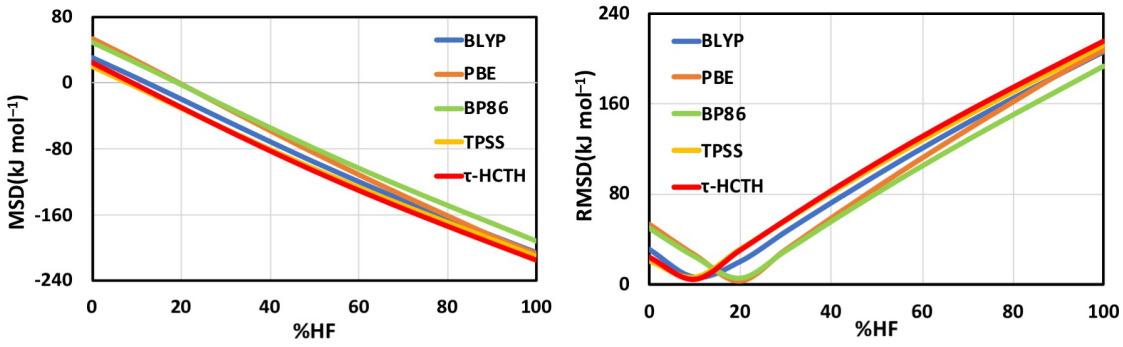

Figure 4. The MSDs and RMSDs over the database on the exact exchange mixing coefficient for three GGA and two MGGA functionals.

The delocalisation error is a sources of error in DFT and is associated with a range of performance issues.[93-94] One way to measure the impact of delocalization error is to construct fractional charge plots as charge is transferred between two species,[95-96] in this case as FAr• and R• become FAr^- and R^+, respectively. Two examples are given in Figure 5 with R = H and CH_2CH. Exact DFT behaviour is expected to show linear dependence with fractional charge.[97] Delocalisation error is characterised by an overstabilization of fractional charge, resulting in concave-up energy curves. HF possesses some localization error resulting in

concave-down energy curves. Clearly, while inclusion of a percentage of HF returns the more 'ideal' linear behaviour, 50% or more HF is required to approach full linearity, far in excess of the optimal percentage identified (indeed, consistent with the more egregious errors identified). This indicates that the hybrid functionals returning good accuracy are likely benefiting from some cancellation of error between their exchange and correlation components. Further, this highlights that while energies calculated using these functionals may be reliable, this does not extend to other properties that can be extracted from the same calculation (such as charge-transfer behaviour).

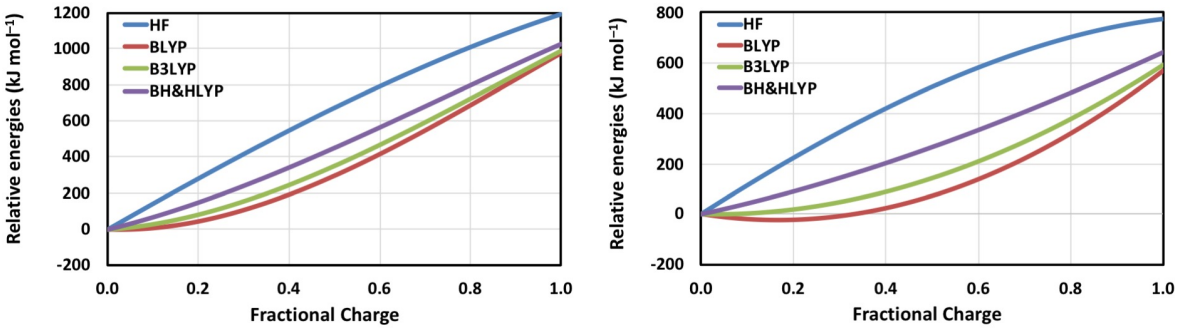

Figure 5. Energy vs. fractional charge plots for R = H (left) and CH_2CH (right) as FAr• and R• transition to FAr^- and R^+. These calculations were conducted using Q-Chem.[98]

Range-separated functionals tend to systematically underestimate BDEs in the NGC14 database. Inspection of the error statistics obtained from the RS procedures reveals that, the RS functionals considered here systematically underestimate the bond dissociation energies in the NGC14 database, as evident from MSD = –1×MAD. Unfortunately, none of the considered RS functionals gives performance with RMSDs below the threshold of chemical accuracy. This might due to the high percentage of exact HF exchange at long range included in these functionals (CAM-B3LYP includes 65% HF exchange at long range, while all the others include 100% HF exchange at long range.).

Double-hybrid functionals show improved performance over conventional hybrids. It has been shown that the DH functionals show good performance for predicting isomerization energies in conjugated dienes[99] and enones,[100] with RMSDs below the threshold of chemical accuracy. Here we concentrate on the performance of the non-dispersion-corrected functionals, and the ones with dispersion correction will be discussed in the next section. All the considered DH procedures except for B2K-PLYP tend to overestimate the bond dissociation energies in the NGC14 database. Four (B2GP-PLYP, B2K-PLYP, B2T-PLYP and PWPB95) out of the considered seven DH procedures result in RMSDs below 4.0 kJ mol^{-1}. While, B2-PLYP, DSD-BLYP, and DSD-PBEP86 give RMSDs of 12.0, 12.9 and 15.9 kJ mol^{-1}, respectively. Remarkably, the B2T-PLYP with 60% of exact HF exchange gives the best performance with an RMSD of merely 2.5 kJ mol^{-1}, while DSD-PBEP86 with 70% of exact HF exchange shows the worst performance with an RMSD of 15.9 kJ mol^{-1}.

Dispersion corrections. Table S2 of the Supporting Information gives the contributions of the D3 dispersion corrections to the 14 bond dissociation reactions. It is obvious that dispersion corrections tend to stabilize the bond dissociation. The magnitude of the dispersion correction ranges from 0.2 to 13.4 kJ mol^{-1} and universally increase the BDEs. As most of the DFT functionals from rungs 2–3 of Jacob's Ladder tend to overestimate the BDEs, inclusions of the dispersion correction almost always worsen the performance of the DFT procedures. Thus, there is no point in including the D3 dispersion corrections as they can only increase the deviations. Table 3 gathers the differences in RMSD between the dispersion-corrected and uncorrected DFT functionals (ΔD3 = RMSD(DFT-D3) – RMSD(DFT)). A negative ΔD3 value indicates that the dispersion correction improves the performance of the functional, while a positive number indicates deterioration in performance.

Inspection of Table 3 reveals that adding dispersion D3 corrections for most of the considered functionals deteriorates the performance of the DFT methods, In particular, the PMSDs are increased by amounts ranging from 0.1 (PW6B95) to 12.2 (BLYP) kJ mol^{-1}. For the range-separated functionals, adding dispersion D3 corrections improves the agreement with the CCSD(T)/CBS reference values. Finally, it is worth pointing out that as all the considered DH functionals overestimate the BDEs in the NGC14 dataset, the performance of these functionals are deteriorated upon inclusion of the D3 dispersion correction. In particular, the RMSDs are increased by amount of 4.1 (DSD-PBEP86) and 6.5 (B2-PLYP) kJ mol^{-1}.

Table 3. Overview of the performance of various DFT functionals with and without D3 dispersion correction.[a]

Type	Method	ΔD3[b]
GGA	BLYP	12.2
	PBE	5.9
	BP86	9.9
MGGA	TPSS	7.5
HGGA	BH&HLYP	-8.1
	B3LYP	8.1
	B3PW91	9.5
	PBE0	1.4
HMGGA	BMK	-6.7
	B1B95	4.5
	PW6B95	0.1
RS	CAM-B3LYP	-5.1
	LC-wPBE	-6.1
DH	B2-PLYP	6.5
	B2GP-PLYP	3.7
	DSD-PBEP86	4.1
	PWPB95	2.6

[a]Footnotes a-c to Table 2 apply here.
[b]ΔD3 = RMSD(DFT-D3) – RMSD(DFT).

3.3 Performance of composite ab initio procedures

Table 4 lists an overview of the performance of the composite procedures, including G3, G3MP2, G3B3, G3MP2B3, G4, G4(MP2), G4(MP2)-6X and CSB-QB3. It has been shown that the G3-type and G4-type procedures give excellent performance for predicting isomerization energies in dienes[99] and enones,[100] with RMSDs < 2.0 kJ mol^{-1}. The G4-type methods have also been reported to give good performance for reaction energies in cycloreversion reactions,[101] resulting RMSDs below 4.0 kJ mol^{-1}. However, upon inspection of the results for the composite procedures, a few interesting features emerge. None of the G*n*-type procedures results in RMSDs below the chemical accuracy threshold except for G4(MP2)-6X. The G3-type procedures exhibit similar performance as G4-type with RMSDs ranging between 5.0 and 9.9 kJ mol^{-1}. G3B3 and G3MP2B3 give better performance than G3 and G3MP2. The G4-type procedures show a disappointing performance except for G4(MP2)-6X, which results in an RMSD of 3.3 kJ mol^{-1}. The CBS-QB3 procedure has been shown to give excellent performance for the barrier heights and reaction energies in cycloreversion reactions as well as isomerization energies in dienes and enones.[99-102] While the CBS-QB3 procedure here obtains a high RMSD of 6.9 kJ mol^{-1} for the NGC14 dataset. This indicates the importance of benchmarking the performance of empirical composite procedures for specific reaction types and systems prior to applying them for the calculation of bond dissociation energies. Finally, we note that most of the composite procedures tend to overestimate the bond dissociation energies in the NGC14 dataset while G3B3 and G4 underestimate them.

Table 4. Statistical analysis for the performance of composite methods for the calculation of the bond dissociation energies in the NGC14 dataset (in kJ mol^{-1}).[a]

Methods	RMSD	MAD	MSD	LD
G3	8.1	7.7	4.7	13.0(1)
G3MP2	9.9	9.5	6.6	15.2(15)
G3B3	5.0	3.4	-2.1	12.7(2)
G3MP2B3	6.7	6.2	4.1	9.8(9)
G4	11.7	6.8	-4.5	31.3(10)
G4(MP2)	9.2	8.7	8.7	12.5(9)
G4(MP2)-6X	3.3	2.6	0.5	6.9(2)
CBS-QB3	6.9	6.7	4.8	8.4(9)

[a]Footnotes b and d to Table 2 apply here.

4. Conclusions

We have obtained benchmark bond dissociation energies by means of the high-level W1 composite thermochemistry protocols for the NGC14 database. We use these benchmark BDEs to evaluate the performance of a variety of contemporary density functional theory and composite procedures. We find that the BDEs in the database are a challenging test for most conventional DFT procedures. With regard to the performance of the DFT and DHDFT functionals we make the following observations:

- The GGA functionals universally overestimate the bond dissociation energies. The RMSDs for the functionals without D3 dispersion correction range between 30.9 (HCTH407) and 67.5 (PBE) kJ mol^{-1}. The functionals with D3 dispersion correction result in RMSDs ranging from 43.1 (B97-D3) to 73.4 (PBE-D3) kJ mol^{-1}. Thus, GGA functionals are not recommended for calculating bond dissociation energies in the NGC14 database.
- The MGGA functionals lead to slightly better performance but still systematically overestimate the BDEs. The best performing MGGAs are M06-L and VSXC with RMSD of 5.4 and 6.4 kJ mol^{-1}, respectively.

- The HGGA and HMGGA functionals tend to underestimate the BDEs, in such case inclusion of D3 dispersion correction can significantly improve the performance. Functionals with 10–28% of exact HF exchange perform better than the ones with more than 28% of exact HF exchange. The best performing methods are B3LYP (4.7), B3PW91 (4.9), and M06 (2.9), and B1B95 (2.7 kJ mol^{-1}).
- The RS functionals tend to underestimate the bond dissociation energies. Only two functionals (CAM-B3LYP-D3 and M11) result in RMSDs below 10.0 kJ mol^{-1}.
- The DHDFT procedures give excellent performance except for B2-PLYP, B2-PLYP-D3, DSD-BLYP, and DSD-PBEP86. The best performing functional is B2T-PLYP with an RMSD of 2.5 kJ mol^{-1}.

Overall, we suggest that for computing accurate bond dissociation energies, an appropriate choice of hybrid or double-hybrid functionals should be used.

With regard to the performance of the composite procedures, we draw the following conclusions:

- The NGC14 database proves to be a challenging test for nearly all of the composite procedures, resulting RMSDs of up to 11.7 kJ mol^{-1}.
- The G*n*-type procedures show moderate performance with RMSDs ranging from 3.3 (G4(MP2)-6X) to 11.7 (G4) kJ mol^{-1}.
- The CBS-QB3 method shows slightly better performance yielding an RMSD of 6.9 kJ mol^{-1}.

Acknowledgments

We gratefully acknowledge the generous allocation of computing time from the National Computational Infrastructure (NCI) Facility and the system administration support provided

by the Faculty of Science at UWA to the Linux cluster of the Karton group. AK gratefully acknowledges an Australian Research Council (ARC) Future Fellowship (Project No. FT170100373).

References

1. L. Pauling, *Journal of the American Chemical Society* **1933,** *55*, 1895-1900.
2. N. Bartlett, *Proceedings of the Chemical Society* **1962**, 218.
3. L. Y. Nelson; G. C. Pimentel, *Inorganic Chemistry* **1967,** *6*, 1758-1759.
4. S. Seidel; K. Seppelt, *Science* **2000,** *290*, 117-118.
5. M. Pettersson; J. Lundell; M. Räsänen, *European Journal of Inorganic Chemistry* **1999,** *1999*, 729-737.
6. J. G. Malm; H. Selig; J. Jortner; S. A. Rice, *Chemical Reviews* **1965,** *65*, 199-236.
7. C. T. Goetschel; K. R. Loos, *Journal of the American Chemical Society* **1972,** *94*, 3018-3021.
8. L. J. Turbini; R. E. Aikman; R. J. Lagow, *Journal of the American Chemical Society* **1979,** *101*, 5833-5834.
9. L. Stein; J. R. Norris; A. J. Downs; A. R. Minihan, *Journal of the Chemical Society, Chemical Communications* **1978**, 502-504.
10. R. D. LeBlond; D. D. DesMarteau, *Journal of the Chemical Society, Chemical Communications* **1974**, 555-556.
11. J. Turner; G. C. Pimentel, *Science* **1963,** *140*, 974-975.
12. J. C. Sanders; G. J. Schrobilgen, *Journal of the Chemical Society, Chemical Communications* **1989**, 1576-1578.
13. K. S. Pitzer, *Journal of the Chemical Society, Chemical Communications* **1975**, 760b-761.
14. V. V. Avrorin; R. N. Krasikova; V. D. Nefedov; M. A. Toropova, *Russian Chemical Reviews* **1982,** *51*, 12.
15. L. Khriachtchev; M. Pettersson; N. Runeberg; J. Lundell; M. Räsänen, *Nature* **2000,** *406*, 874.
16. A. J. Cohen; P. Mori-Sánchez; W. Yang, *Chemical Reviews* **2011,** *112*, 289-320.
17. A. E. Mattsson, *Science* **2002,** *298*, 759-760.
18. R. Car, *Nature Chemistry* **2016,** *8*, 820.
19. J. Sun; R. C. Remsing; Y. Zhang; Z. Sun; A. Ruzsinszky; H. Peng; Z. Yang; A. Paul; U. Waghmare; X. Wu, *Nature Chemistry* **2016,** *8*, 831.
20. J. P. Perdew; A. Ruzsinszky; J. Tao; V. N. Staroverov; G. E. Scuseria; G. I. Csonka, *The Journal of Chemical Physics* **2005,** *123*, 062201.
21. E. R. Johnson; O. J. Clarkin; G. A. DiLabio, *The Journal of Physical Chemistry A* **2003,** *107*, 9953-9963.
22. E. I. Izgorodina; M. L. Coote; L. Radom, *The Journal of Physical Chemistry A* **2005,** *109*, 7558-7566.
23. B. Chan; L. Radom, *The Journal of Physical Chemistry A* **2012,** *116*, 4975-4986.
24. R. J. O'Reilly; A. Karton; L. Radom, *International Journal of Quantum Chemistry* **2012,** *112*, 1862-1878.
25. R. J. O'Reilly; A. Karton, *International Journal of Quantum Chemistry* **2016,** *116*, 52-60.
26. A. Karton; S. Daon; J. M. L. Martin, *Chemical Physics Letters.* **2011,** *510*, 165-178.
27. R. Gerber, *Annual Review Physical Chemistry* **2004,** *55*, 55-78.
28. J. M. Martin, *Annual Reports in Computational Chemistry* **2005,** *1*, 31-43.
29. A. Karton, *Wiley Interdisciplinary Reviews: Computational Molecular Science* **2016,** *6*, 292-310.

30. H. Werner; P. Knowles; G. Knizia; F. Manby; M. Schütz; P. Celani; W. Györffy; D. Kats; T. Korona; R. Lindh; e. al, *MOLPRO is a package of ab initio programs*, version 2012.1; 2012.
31. J. M. Martin; S. Parthiban, W1 and W2 theories, and their variants: thermochemistry in the kJ/mol accuracy range. In *Quantum-Mechanical Prediction of Thermochemical Data*, Springer: 2001; pp 31-65.
32. J. M. Martin; G. de Oliveira, *The Journal of Chemical Physics* **1999,** *111*, 1843-1856.
33. T. H. Dunning Jr, *The Journal of Chemical Physics* **1989,** *90*, 1007-1023.
34. R. A. Kendall; T. H. Dunning; R. J. Harrison, *The Journal of Chemical Physics* **1992,** *96*, 6796.
35. T. H. Dunning Jr; K. A. Peterson; A. K. Wilson, *The Journal of Chemical Physics* **2001,** *114*, 9244-9253.
36. K. A. Peterson; T. H. Dunning Jr, *The Journal of Chemical Physics* **2002,** *117*, 10548-10560.
37. C. Lee; W. Yang; R. G. Parr, *Physical Review B* **1988,** *37*, 785.
38. A. D. Becke, *The Journal of Chemical Physics* **1993,** *98*, 5648-5652.
39. P. Stephens; F. Devlin; C. Chabalowski; M. J. Frisch, *The Journal of Physical Chemistry* **1994,** *98*, 11623-11627.
40. S. Grimme; S. Ehrlich; L. Goerigk, *Journal of Computational Chemistry* **2011,** *32*, 1456-1465.
41. S. Grimme; J. Antony; S. Ehrlich; H. Krieg, *The Journal of Chemical Physics* **2010,** *132*, 154104.
42. S. Grimme, *Wiley Interdisciplinary Reviews: Computational Molecular Science* **2011,** *1*, 211-228.
43. A. D. Becke; E. R. Johnson, *The Journal of Chemical Physics* **2005,** *123*, 154101.
44. S. Grimme, *Journal of Computational Chemistry* **2006,** *27*, 1787-1799.
45. M. Frisch; G. Trucks; H. Schlegel; G. Scuseria; M. Robb; J. Cheeseman; G. Scalmani; V. Barone; G. Petersson; H. Nakatsuji; e. al., Gaussian 09. Revision E. 01. Gaussian Inc., Wallingford, CT, USA. 2009.
46. A. D. Becke, *Physical Review A* **1988,** *38*, 3098.
47. A. D. Boese; N. C. Handy, *The Journal of Chemical Physics* **2001,** *114*, 5497-5503.
48. J. P. Perdew; K. Burke; M. Ernzerhof, *Physical Review Letters* **1996,** *77*, 3865.
49. J. P. Perdew, *Physical Review B* **1986,** *33*, 8822.
50. J. P. Perdew; J. A. Chevary; S. H. Vosko; K. A. Jackson; M. R. Pederson; D. J. Singh; C. Fiolhais, *Physical Review B* **1992,** *46*, 6671.
51. R. Peverati; Y. Zhao; D. G. Truhlar, *The Journal of Physical Chemistry Letters* **2011,** *2*, 1991-1997.
52. R. Peverati; D. G. Truhlar, *Journal of Chemical Theory and Computation* **2012,** *8*, 2310-2319.
53. Y. Zhao; D. G. Truhlar, *The Journal of Chemical Physics* **2006,** *125*, 194101.
54. J. Tao; J. P. Perdew; V. N. Staroverov; G. E. Scuseria, *Physical Review Letters* **2003,** *91*, 146401.
55. A. D. Boese; N. C. Handy, *The Journal of Chemical Physics* **2002,** *116*, 9559-9569.
56. T. Van Voorhis; G. E. Scuseria, *The Journal of Chemical Physics* **1998,** *109*, 400-410.
57. A. D. Becke, *The Journal of Chemical Physics* **1996,** *104*, 1040-1046.
58. R. Peverati; D. G. Truhlar, *The Journal of Physical Chemistry Letters* **2011,** *3*, 117-124.
59. R. Peverati; D. G. Truhlar, *Physical Chemistry Chemical Physics* **2012,** *14*, 13171-13174.

60. A. D. Becke, *Journal of Chemical Physics* **1993,** *98*, 1372-1377.
61. C. Adamo; V. Barone, *Journal of Chemical Physics* **1999,** *110*, 6158-6170.
62. S. H. Kim; S. D. Yoh; C. Lim; M. Mishima; M. Fujio; Y. Tsuno, *Journal of Physical Organic Chemistry* **1998,** *11*, 254-260.
63. H. L. Schmider; A. D. Becke, *The Journal of Chemical Physics* **1998,** *108*, 9624-9631.
64. X. Xu; Q. Zhang; R. P. Muller; W. A. Goddard III, *The Journal of Chemical Physics* **2005,** *122*, 014105.
65. R. Peverati; D. G. Truhlar, *The Journal of Chemical Physics* **2011,** *135*, 191102.
66. Y. Zhao; N. E. Schultz; D. G. Truhlar, *The Journal of Chemical Physics* **2005,** *123*, 161103.
67. Y. Zhao; N. E. Schultz; D. G. Truhlar, *Journal of Chemical Theory and Computation* **2006,** *2*, 364-382.
68. Y. Zhao; D. G. Truhlar, *Theoretical Chemistry Accounts* **2008,** *120*, 215-241.
69. A. D. Boese; J. M. Martin, *The Journal of Chemical Physics* **2004,** *121*, 3405-3416.
70. V. N. Staroverov; G. E. Scuseria; J. Tao; J. P. Perdew, *The Journal of Chemical Physics* **2003,** *119*, 12129-12137.
71. Y. Zhao; D. G. Truhlar, *The Journal of Physical Chemistry A* **2005,** *109*, 5656-5667.
72. S. Grimme, *The Journal of Chemical Physics* **2006,** *124*, 034108.
73. A. Karton; A. Tarnopolsky; J.-F. Lamére; G. C. Schatz; J. M. Martin, *The Journal of Physical Chemistry A* **2008,** *112*, 12868-12886.
74. A. Tarnopolsky; A. Karton; R. Sertchook; D. Vuzman; J. M. Martin, *The Journal of Physical Chemistry A* **2008,** *112*, 3-8.
75. S. Kozuch; D. Gruzman; J. M. L. Martin, *The Journal of Physical Chemistry C* **2010,** *114*, 20801-20808.
76. S. Kozuch; J. M. L. Martin, *Physical Chemistry Chemical Physics* **2011,** *13*, 20104-20107.
77. S. Kozuch; J. M. L. Martin, *Journal of Computational Chemistry* **2013,** *34*, 2327-2344.
78. L. Goerigk; S. Grimme, *Journal of Chemical Theory and Computation* **2011,** *7*, 291-309.
79. T. Yanai; D. P. Tew; N. C. Handy, *Chemical Physics Letters* **2004,** *393*, 51-57.
80. O. A. Vydrov; G. E. Scuseria, *The Journal of Chemical Physics* **2006,** *125*, 234109.
81. J. D. Chai; M. Head-Gordon, *The Journal of Chemical Physics* **2008,** *128*, 084106.
82. J. D. Chai; M. Head-Gordon, *Physical Chemistry Chemical Physics* **2008,** *10*, 6615.
83. R. Peverati; D. G. Truhlar, *The Journal of Physical Chemistry Letters* **2011,** *2*, 2810-2817.
84. L. A. Curtiss; K. Raghavachari; P. C. Redfern; V. Rassolov; J. A. Pople, *The Journal of Chemical Physics* **1998,** *109*, 7764-7776.
85. L. A. Curtiss; P. C. Redfern; K. Raghavachari; V. Rassolov; J. A. Pople, *The Journal of chemical physics* **1999,** *110*, 4703-4709.
86. A. G. Baboul; L. A. Curtiss; P. C. Redfern; K. Raghavachari, *The Journal of Chemical Physics* **1999,** *110*, 7650-7657.
87. L. A. Curtiss; P. C. Redfern; K. Raghavachari, *The Journal of Chemical Physics* **2007,** *126*, 084108.
88. L. A. Curtiss; P. C. Redfern; K. Raghavachari, *The Journal of Chemical Physics* **2007,** *127*, 124105.
89. B. Chan; J. Deng; L. Radom, *Journal of Chemical Theory and Computation* **2011,** *7*, 112-120.

90. J. A. Montgomery; M. J. Frisch; J. W. Ochterski; G. A. Petersson, *The Journal of Chemical Physics* **1999,** *110*, 2822.
91. A. Karton; E. Rabinovich; J. M. Martin; B. Ruscic, *The Journal of Chemical Physics* **2006,** *125*, 144108.
92. X. Zhang; H. Schwarz, *Theoretical Chemistry Accounts* **2011,** *129*, 389-399.
93. C. Li; X. Zheng; N. Q. Su; W. Yang, *National Science Review* **2017,** *5*, 203-215.
94. J. L. Bao; Y. Wang; X. He; L. Gagliardi; D. G. Truhlar, *The Journal of Physical Chemistry Letters* **2017,** *8*, 5616-5620.
95. A. J. Cohen; P. Mori-Sánchez; W. Yang, *Science* **2008,** *321*, 792-794.
96. E. R. Johnson; A. Otero-de-la-Roza; S. G. Dale, *The Journal of Chemical Physics* **2013,** *139*, 184116.
97. J. P. Perdew; R. G. Parr; M. Levy; J. L. Balduz Jr, *Physical Review Letters* **1982,** *49*, 1691.
98. Y. Shao; Z. Gan; E. Epifanovsky; A. T. Gilbert; M. Wormit; J. Kussmann; A. W. Lange; A. Behn; J. Deng; X. Feng; e. al., *Molecular Physics* **2015,** *113*, 184-215.
99. L.-J. Yu; A. Karton, *Chemical Physics* **2014,** *441*, 166-177.
100. L.-J. Yu; F. Sarrami; A. Karton; R. J. O'Reilly, *Molecular Physics* **2015,** *113*, 1284-1296.
101. L.-J. Yu; F. Sarrami; R. J. O'Reilly; A. Karton, *Molecular Physics* **2016,** *114*, 21-33.
102. L.-J. Yu; F. Sarrami; R. J. O'Reilly; A. Karton, *Chemical Physics* **2015,** *458*, 1-8.